Fuel saving of rear based retrofit hybridization from front based engine vehicle

Florian Tournez, Robin Vincent, Walter Lhomme, A Richert, Alain Bouscayrol, Mariam Amhed, Betty Semail, Aurelien Lievre

Fuel saving of rear based retrofit hybridization from front based engine vehicle

F. Tournez[1], R. Vincent[2], W. Lhomme[1], A. Richert[2], A. Bouscayrol[1], M. Ahmed[2], B. Lemaire-Semail[1], A. Lievre[2],

[1]Univ. Lille, Arts et Metiers Institute of Technology, Centrale Lille, Yncrea Hauts-de-France, ULR 2697 - L2EP, F-59000 Lille, France

[2]Valeo Equipements Electriques Moteur, 2 rue André Boulle, Créteil, F-94017 Cedex, France

Email: Walter.Lhomme@univ-lille.fr

***Abstract* – The transformations of conventional Internal Combustion Engine (ICE)-powered vehicles into electrified vehicles are of growing interest. The retrofit hybridization of a Peugeot 308 SW passenger car is studied. For this purpose, a complete hybridization system is added to the rear axle of the vehicle. As a result, the control of the initial ICE-powered vehicle has to be updated. The aim of this paper is to deduce the potential fuel saving thanks to this hybridization. The simulation results show an energy saving of at least 9% and potential consumption reduction on a Worldwide harmonized Light-duty Vehicles Test Cycle (WLTC).**

***Keywords*— Control, Energetic Macroscopic Representation, Hybrid Electric Vehicles, Retrofit, Strategy**

I. Introduction

Nowadays, many solutions are being put in place to deal with global warming. Electrified vehicles are one of them [1]. If new vehicles can be developed in that aim, it is also possible to convert a conventional vehicle into a battery electric vehicle. Since the decree signed in March 2020, the French government authorizes such conversions. However, the implementation of new electrified vehicles in the market will be progressive and a lot of ICE-powered vehicles will carry on to deliver high pollutant emissions. The transformation of these conventional cars into electrified cars (i.e. retrofit) is thus a key challenge when the electrification of the vehicle, the energetic efficiency of the system and the affordable cost for drivers are taken into account.

The aim of this transformation is to reduce fuel consumption and thus mitigate the greenhouse gas emissions. A few vehicle retrofits have already been studied in literature [2][3]. In terms of Hybrid Electric Vehicles (HEV) and Plug Hybrid Electric Vehicles (P-HEV), there exist different topologies: series, parallel and series-parallel [4]. Some concepts today are also based on parallel configuration caused by a quick design and simplified integration into the vehicle [3]. For the retrofitting hybrid system, there exist many places to integrate the electric drive inside the vehicle [5]. The complexity of integration depends directly on the segment of the vehicle and the changes in the transmission.

In this study, a 48V parallel hybrid system is considered by hybridization of the rear axle of a conventional vehicle. This choice is based on the advantage of being totally independent of the front axle and to have a free space under the car trunk. In this way, no modification is made to the already existing transmission and limits the number of important changes in the vehicle. Usage of 48V EM instead of high voltage also aims in that direction. Indeed, no specific safety system is required below 50V.

The objective of this paper is to estimate the fuel saving when converting a classical Peugeot 308 SW in hybrid vehicle. The rear hybridizing system is composed: a low voltage battery, a converter with its water-cooling system, an electrical machine of 15 kW, a dogbox and its on-board charger (OBC). This extension aims to minimize the change in the vehicle keeping the initial front ICE-base powertrain. Moreover, the initial control is just extended by a power distribution function. If thus hybridization is not the most efficient, it enables an easy and low cost conversion.

Section II deals with the characteristic, the model and the control algorithm of the initial ICE vehicle. Section III deals with the integration of the rear electrical drive in the vehicle and its control. Section IV compare the simulation results between the conventional vehicle with its retrofit version.

II. Modelling and Control of the Studied ICE-Powered vehicle

A. Studied Vehicle

The studied vehicle is a classical Peugeot 308 SW (Fig. 1). The main characteristics of the vehicle are listed in Table 1.

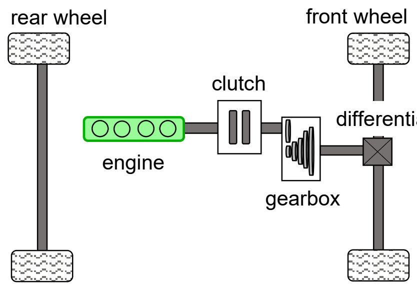

Fig. 1: Structural scheme of the studied vehicle

Some values came from the Peugeot manufacturer datasheet ("M" in the table). Non available has been defined from the test bench experimentation ("E" in the Table).

Table 1 : Vehicle's parameters

Variable	Signification	Value	Unit	Origin
M_{veh}	Curb mass + 1 passenger	1225	kg	M
K_{tr}	Equivalent transmission ratio (gearbox and final drive)	[17.8 8.9 5.75 4.25 3.14 2.47]	/	E
R_{wh}	Wheel radius	0.3068	m	M

A	correlates to the rolling resistance	100.6	N	E
B	relates to the spinning or rotational losses	1.62	$N/m.s^{-1}$	E
C	aerodynamic drag	0.41	$N/m^2.s^{-2}$	
η_{tr}	Gearbox efficiency	0.95	/	M

B. Modelling and EMR of the vehicle

The Energetic Macroscopic Representation (EMR) formalism is used to organize the interconnection of all the models. EMR is a graphical formalism for a description of multi-disciplinary energy systems such as HEV [6]. EMR is based on the principle of interaction and on a macroscopic view of subsystems. It respects the physical causality [7] and a control structure can be systematically derived from the EMR [6]. In this way, the EMR formalism is a good choice to organize the models of the vehicle and deduce its control organization. The formalism is based on four basic pictograms; 1) the source element; 2) the accumulation element; 3) the element conversion element and; 4) the coupling element (see appendix)

1) Internal Combustion Engine (ICE)

The ICE provides the traction power to the transmission. A static model is considered assuming an ideal control:

$$T_{ice} = T_{ice\_ref} \tag{1}$$

The fuel consumption is determined with an efficiency map depending on the engine torque, rotation speed and the water temperature of the cooling system (friction losses).

2) Mechanical transmission

The transmission is composed of an automatic gearbox and a mechanical differential (final drive), described by an equivalent ratio K_{tr}. The coefficient K_{tr} can take 6 different values (discrete gear) in function of the gear engaged. The different ratios have been obtained previously by experimental results on a test bench. Moreover, a constant efficiency coefficient η_{tr} is considered. In reality, the efficiency fluctuates depending on the gear engaged, the speed and the torque. The clutch is neglected because it has a few impacts on the consumption [[5]. The transmission torque T_{tr} and rotation speed Ω_{ice} are obtained by the following equations:

$$\begin{cases} T_{tr} = T_{ice} K_{tr} \eta_{tr}^{\gamma_{tr}} \\ \Omega_{ice} = \Omega_{tr} K_{tr} \end{cases} \tag{2}$$

$$\text{with: } \begin{cases} \gamma_{tr} = 1 & \text{if } T_{ice} \geq 0 \\ \gamma_{tr} = -1 & \text{if } T_{ice} < 0 \end{cases}$$

3) Wheel

Only straight lines are assumed as the effect of the turns on the fuel consumption is very low. Therefore, an equivalent wheel is considered [9]. The force F_{wh} at the wheel is obtained directly from the radius of the wheel R_{wh} and in the same way for the rotation speed of the transmission Ω_{tr}:

$$\begin{cases} F_{wh} = \dfrac{T_{tr}}{R_{wh}} \\ \Omega_{tr} = \dfrac{v_{wh}}{R_{wh}} \end{cases} \tag{3}$$

4) Mechanical braking

A mechanical braking leads to a braking force F_{brk} that is added to the wheel force F_{wh} to obtain the total force F_{tot}:

$$\begin{cases} F_{tot} = F_{wh} - F_{brk} \\ v_{veh} = v_{brk} = v_{wh} \end{cases} \tag{4}$$

5) Mechanical brake

The mechanical brake is represented by a source pictogram (green oval) with an ideal control (no delay).

$$F_{brk\_ref} = F_{brk} \tag{5}$$

6) Chassis

The chassis defines the velocity of the vehicle as a function of the total force of traction F_{tot} and the resistance force F_{res}. The different inertias of the vehicle are neglected in a first step. The mass of the vehicle M_{veh} is related to the curb mass added with a passenger mass.

$$M_{veh} \frac{d_{veh}}{dt} = F_{tot} - F_{res} \tag{6}$$

7) Environnement

In this study, the wind and the slopes are not considered. The resistive force F_{res} can thus be expressed as follows (7). Coefficient *A* is related to the rolling resistance, coefficient *B* to the spinning or rotational losses and *C* to the aerodynamic drag [9].

$$F_{res} = A + B\, v_{veh} + C\, v_{veh}^2 \tag{7}$$

The EMR of the vehicle is deduced from the modeling equation (Fig. 2). The model of the vehicle is represented with different pictograms. The source element pictograms are represented with a green oval at the extremity of the model corresponding to the ICE, the mechanical brake and the environment. The orange square element (energy conversion element without energy storage) matches with the transmission and the wheel. The double orange square (coupling element) allows to distribute energy in the different elements. In this case, it stands to couple the brakes with the wheel. Finally, the orange crossed rectangular (accumulation element i.e. energy storage) is linked with the chassis of the vehicle. The model shows 3 red arrows as tuning inputs: T_{ice_ref} corresponds to the engine torque reference, K_{gb_ref} corresponds to the gear engaged and the F_{brk_ref} corresponds to the braking force reference. These different references will be defined by the Energy Management Strategy (EMS) or the driver (gear ratio).

A. Control scheme

The EMR properties allow to deduce the control of the system synthetically using a mirror effect [6] (Fig. 3). The inversion of the chassis requires a closed-loop control using a controller *C(t)*:

$$F_{tot\_ref} = \left(v_{veh\_ref} - v_{veh\_mea}\right) C(t) + F_{res\_mea} \tag{8}$$

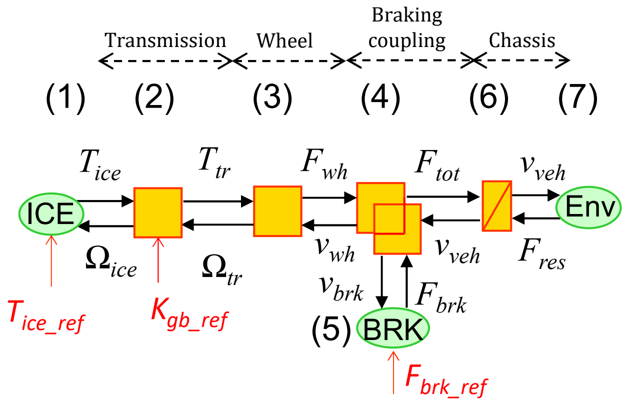

Fig. 2: EMR of the studied engine-powered vehicle

The inversion of the coupling element allows to share the braking force F_{brk_ref} and the traction force F_{wh_ref}:

$$\begin{cases} F_{wh\_ref} = F_{tot\_ref} - F_{brk\_ems} \\ F_{brk\_ref} = F_{brk\_ems} \end{cases} \qquad (9)$$

The transmission torque T_{tr_ref} is obtained from a direct inversion of (3).

$$T_{tr\_ref} = R_{wh} F_{wh\_ref} \qquad (10)$$

Finally, the engine torque reference T_{ice_ref} is obtained from the inversion of (2). Fig. 3 shows the control of the engine-powered vehicle.

$$T_{ice\_ref} = \frac{1}{K_{tr}\, \eta_{tr}^{\gamma_{tr}}} T_{tr\_ref} \qquad (11)$$

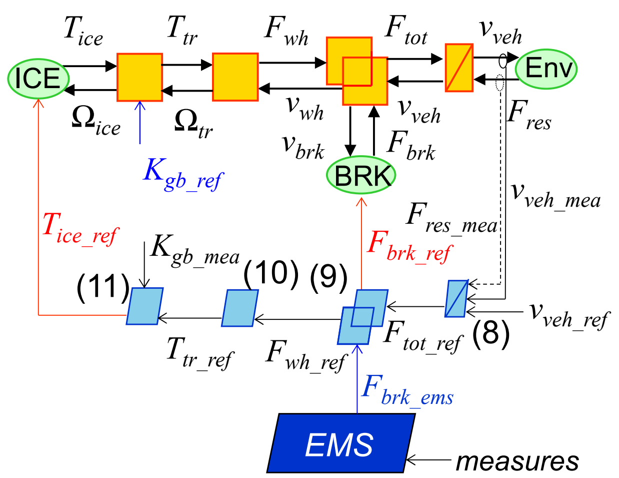

Fig. 3: EMR and control of the studied engine-powered vehicle

III. Retrofit Hybridazion

A. *Studied Hybrid Architecture*

A complete hybridization system (battery, converter, cooling-system, EM, dogbox and OBC) is added to the rear axle of the vehicle so the vehicle becomes a Plug-in Hybrid Electric Vehicle (P-HEV). Fig. 4 show the new architecture of the vehicle and all parameters are listed in Table 2.

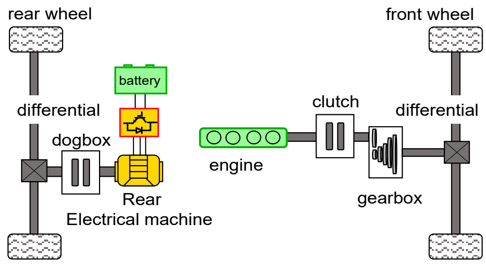

Fig. 4: Selected hybrid architecture

The voltage of 48V makes it possible to be in the safety low voltage range. The advantage is to be able to benefit an electric mode at low speed over a short distance and to be able to recover braking energy. Furthermore, in a conventional vehicle it is possible on average to recover 60% at the front and 40% at the rear of the braking energy [10]. For safety issues related to vehicle stability, we make the assumption stay with this repartition. With this assumption, integrate the EM in front axle seems more interesting. In the most case on the front axle, the EM could be integrated at different positions inside the mechanical transmission excepted for the belt starter generator configuration (BSG). As the BSG configuration does not offer a pure electric mode, this solution is not retained. Moreover, integrate the EM inside the transmission requires to modify the original transmission of the vehicle [5]. This solution can be difficult to implement and more expensive. In this regard, the electric machine is installed at the rear axle of the vehicle at the level of the boot for reasons of simplicity. Additionally, the vehicle would be able to use an all-wheel drive.

Table 2 : Vehicle Parameters (Hybrid System)

Component	**Parameters**	**Mass**
Electrical machine + converter + axis strengthening	15 kW	35 kg
Battery pack	5kWh	40 kg
Rear Reducer K_{trans_rear}	19	20 kg
Others: electrical wire, cooling system, OBC	/	25 kg

The total mass of the hybridization system is 125 kg. The new mass of the vehicle with one passenger is then 1340 kg.

B. *Updating of the modelling and EMR*

The integration of the hybrid system leads to an update of the model.

1) *Electrical drive*

A static model is used for the electric drive (machine, converter and local control) using an efficiency map with T_{em} the machine torque [8].

$$\begin{cases} i_{em} = \dfrac{\Omega_{em}\, T_{em}}{U_{bat}\; \eta_{em}^{\gamma_{em}}} \\ T_{em\_ref} = T_{em} \end{cases} \text{ with } \begin{cases} \gamma_{em} = 1 & \text{if } T_{em} \geq 0 \\ \gamma_{em} = -1 & \text{if } T_{em} < 0 \end{cases} \qquad (12)$$

2) Dogbox & Rear transmission ratio

The dogbox and the rear transmission ratio are described by a single pictogram. The dogbox disconnects the electric machine at high speed to limit mechanical losses. The rear ratio K_{trans_rear} is given by the ratio of the mechanical differential and the gearbox (dual-stage reducer). The rear reducer reduces the speed of the electrical machine. The total losses of the rear transmission are directly given by a torque loss map T_{trans_losses} according to whether dogbox is open or closed (K_{db}) and in function of the speed of the wheel Ω_{db}.

$$\begin{cases} T_{db} = T_{em}\, K_{db}\, K_{trans\_rear} - T_{trans\_losses} \\ \Omega_{em} = \Omega_{db}\, K_{db}\, K_{trans\_rear} \end{cases}$$

$$\text{With: } \begin{cases} k_{db} = 1 \text{ if open} \\ k_{db} = 0 \text{ if closed} \end{cases}$$

3) Wheel

The same relationship as the front wheel is used with F_{wh_re} the force at the wheel, T_{db} the torque at the end of the dogbox, v_{wh_re} the velocity of the vehicle and Ω_{db} the rotational speed of the shaft of the dogbox.

$$\begin{cases} F_{wh\_re} = \dfrac{T_{db}}{R_{wh}} \\ \Omega_{db} = \dfrac{v_{wh\_re}}{R_{wh}} \end{cases} \quad (14)$$

4) Mechanical coupling

The mechanical coupling corresponds in addition to the force produced by the front F_{wh_fr} and rear axle F_{wh_re}. The coupling is created by the chassis to give the final speed.

$$\begin{cases} F_{tot} = F_{wh\_re} + F_{wh\_fr} \\ v_{veh} = v_{wh\_fr} = v_{wh\_re} \end{cases} \quad (15)$$

The global EMR of the vehicle is obtain (Fig. 5) with the unchanged part of the conventional vehicle (grey part). We assume that only the front mechanical brake will be used and that the rear braking will be provided by the electric drive. A more complete study can be realized in further work.

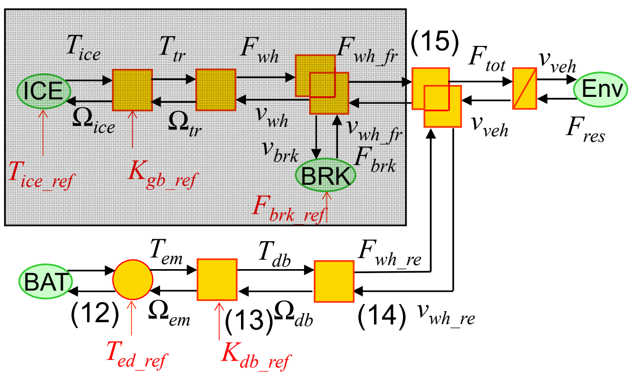

Fig. 5: EMR of the considered HEV

C. Updated control scheme

A new control scheme is deduced from the inversion of the model (Fig. 6). It is important to notice that the control of the conventional vehicle is kept unchanged (grey area in Fig. 6). The new control scheme is coupled with initial control by means of inputs and outputs outside of the grey area. In this way, it is only possible to act on the inputs $F_{wh\_fr\_ref}$ and F_{brk_ems} and the output T_{ice_ref}. The new control equations are given below (16,17,18):

$$\begin{cases} F_{wh\_fr\_ref} = F_{tot\_ref} - F_{wh\_re\_ems} \\ F_{wh\_re\_ref} = F_{wh\_re\_ems} \end{cases} \quad (16)$$

$$T_{db\_ref} = F_{wh\_re\_ref}\, R_{wh} \quad (17)$$

$$T_{ed\_ref} = T_{db\_ref}\, K_{db\_mea} \frac{1}{K_{trans\_rear}} + T_{trans\_losses} \quad (18)$$

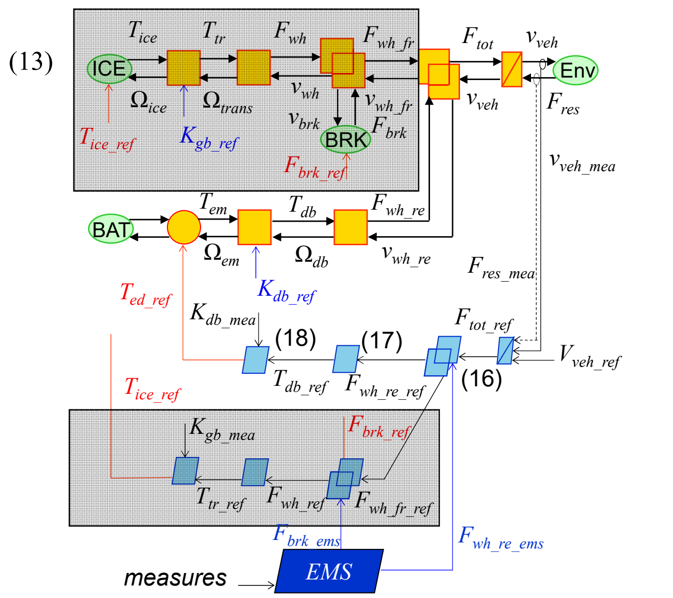

Fig. 6: EMR and control algorithm of the considered HEV

IV. Simulation Results

A. Fuel consumption of the conventional vehicle

Fig. 7 shows the velocity of the vehicle and the fuel consumption along the WLTC class 3b. The WLTC is made up of different areas: downtown, urban, suburban and highway. The total distance of the cycle is 23.2 km. The fuel consumption of the conventional vehicle along the WLTC is 5.86 l/100 km in the simulation. The reference value obtained on the test bench experimentation is 5.97 l/100 km allowing to validate the model in thermal mode.

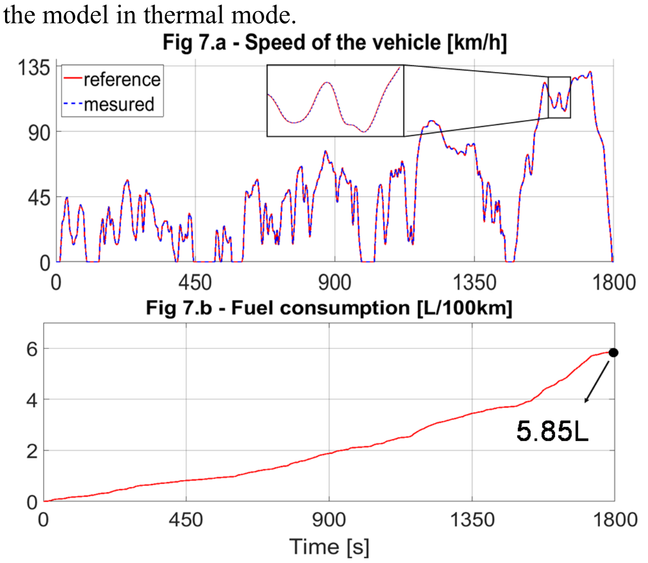

Fig. 7: Result of simulation - Conventional vehicles

B. *Fuel consumption of the studied HEV*

The fuel consumption in a pure ICE operating mode is 6.15 l/100 km in the simulation with the rear hybridization system. Indeed, as the vehicle mass has increased due to the hybridization, the energy consumption only using the ICE has also increased (4 % more). Most of the retrofit cases used rule-based Energy Management Strategy (EMS) because of its facility of implementation caused by a minimalist approach [11]. Therefore, a simple rule-based EMS is defined. The traction EMS flowchart is presented in Fig. 9. The traction force F_{tract} corresponds to the positive value of the force F_{tot_ref} (Fig. 6)

- If the speed is lower than 30 km/h and the state of charge of the battery (SOC) is greater than 20%, the vehicle is in pure electric operation mode.
- If the speed is included between 30 km/h and 70 km/h and the SOC is greater than 20%, the vehicle is in hybrid operation mode
- If the speed is greater than 70 km/h or the SOC is lower than 20 %, the vehicle is in pure ICE operation mode

The conditions to delimit the different operating modes are arbitrary. These are simple limits to highlight the different possible modes. A strategy also based on a boost assistance or with a power limit will be more relevant but more complex to achieve. It will be proposed in a further step.

On the WLTC, the distance covered at low speed (lower than 30 km/h) is about 6 km. In this context, it is possible to benefit from an all-electric low-speed mode and the vehicle could drive along about 34 km in electric mode with a SOC between 95% and 20%.

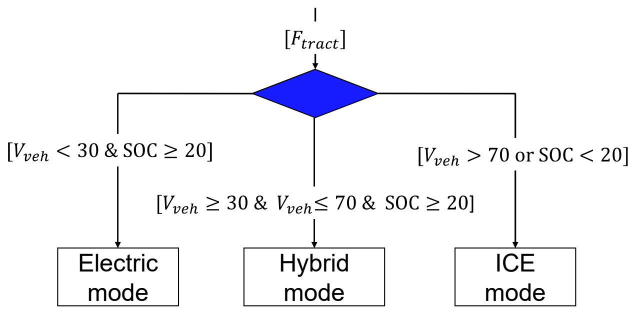

Fig. 8: Traction energy management strategy

The second part of the strategy is the braking EMS. It can then be assumed that 40% of the total braking energy can be recovered by electrification of the rear. This EMS is then managed as follows (Fig. 10). The braking force F_{brk_rear} corresponds to 40% of the negative value of the force F_{tot_ref} (Fig. 6).

- When the speed v_{veh} is lower than 10 km/h and greater than 90 km/h or SOC equal to 100%, a pure mechanical braking is applied (in this velocity range the energy recovery is limited by the electrical machine [10] and dog-box).

- When the speed is included between 10 km/h and 90 km/h, the force F_{em_brk} deduced from the maximal torque of the machine is lower than braking force F_{brk_rear} and the battery SOC is lower than 100%, all rear energy can be recovered.

- When the speed is included between 10 km/h and 90 km/h, the force F_{em_brk} deduced from the torque of the EM is greater than braking force F_{brk_rear} and the battery SOC is lower than 100%, the maximal energy will be recovered (defined by the machine power limit) and the excess energy will be dissipated into the mechanical brakes. It corresponds to a hybrid braking.

The remaining 60% of energy in the front wheels are dissipated with mechanical breaking.

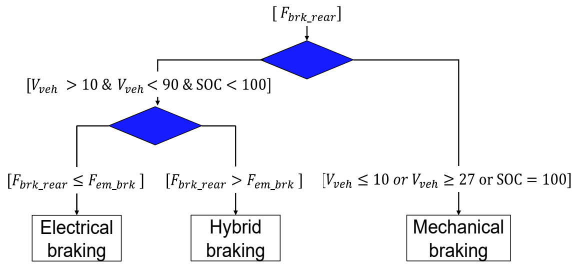

Fig. 9: Braking energy management strategy

Fig. 10 presents the simulation results from the HEV vehicle. Fig. 10.a show the traction power of the electrical machine and traction power of the ICE. Fig. 10.b shows the mechanical and electrical braking power. At low velocity, the braking is only mechanical. In contrast at high velocity, the braking is hybrid and recharge the battery (Fig. 10.b). Respectively, Fig. 10.c and the Fig. 10.d demonstrates the evolution of the SOC the battery and the consumption. The electrification of the vehicle can reduce the fuel consumption to 5.16 l/100 km with a final SOC of 82% (need external recharge). It sure that a fair comparison requires a final SOC equal to the initial SOC. But it is not possible to recharge the battery with ICE with this architecture. Other architectures with the possibility of charging the battery by the ICE could thus be of interest.

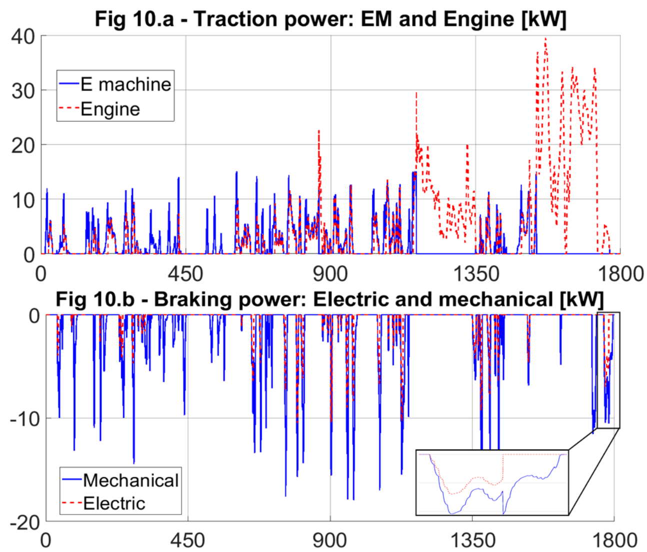

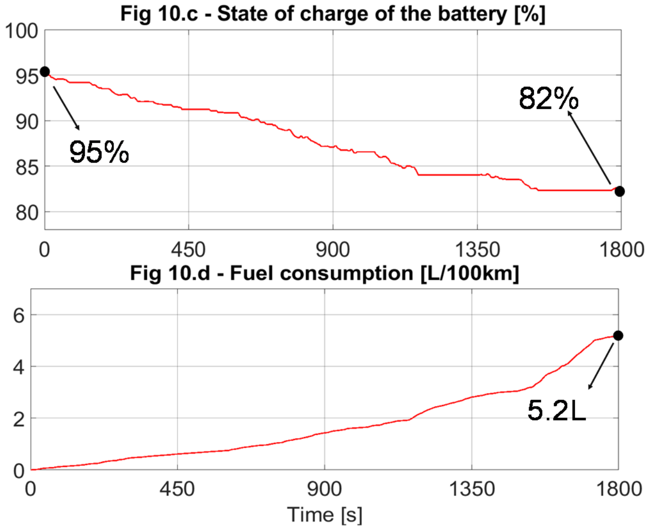

Fig. 10: Result of simulation –HEV vehicle

C. *Comparisons and potential gains*

The study shows that the added mass of the hybrid system leads to an additional 4% fuel consumption (full ICE mode) compared to the conventional vehicle. Through the retrofit, it can reduce the fuel consumption by at least 9 % using electrical energy from the battery and a very simple EMS. One liter of gasoline represents 9.63 kWh. For 100 km, the conventional vehicle consumes then 53.43 kWh. Through the electrical energy, it is possible to reduce the consumption at 52.21 kWh (49.7 kWh from the engine and 2.52 kWh from the batterie). Finally, it is possible to conclude an energy saving of 8% and a CO_2 reduction of 8% at the scale of the vehicle. More energy savings could be envisaged with a more advanced EMS [8][12] and a more compact system (lighter). A more specific driving cycle could be used to see more closely the fuel and energy savings [11].

V. Conclusion

A conventional ICE powered-vehicle has been retrofitted into a P-HEV in a very simple way without changing the initial architecture and control. For the simplicity, an electric drive has just been added on the rear axle of the vehicle without change on the ICE-based mechanical transmission in the front. The vehicle control has just been extended with a distribution strategy keeping the initial ICE control.

A very simple rule-based EMS has been developed that globally leads to a fuel saving of the vehicle. Despite the mass increase, a pure electric traction is possible and also regenerative braking. But a more advanced EMS is required to define the maximal potential gain in terms of energy consumption.

However, this first study demonstrates that even for this very simple architecture and without strong changes, this retrofit can contribute to a fuel saving and a reduction of the CO_2 emission.

In further steps, the investment costs of such a simple hybridization will be studied. Another architecture will also be studied. Particular attention will be paid on the battery capacity.

Acknowledgment

This paper has been realized within the framework of the PANDA project which has received funding from the European Union's Horizon 2020 research and innovation program under grant agreement no. 824256 (PANDA).

References

[1] "Global EV outlook 2018, towards cross-modal electrification", International Energy Agency report, 2018.

[2] S. A. Zulkifli, N. Saad, S. Mohd, et A. R. A. Aziz, « Split-parallel in-wheel-motor retrofit hybrid electric vehicle », in *2012 IEEE International Power Engineering and Optimization Conference*, Melaka, Malaysia, June 2012, pp. 11-16

[3] R. Kumar, A.S Kaundinya, R Shah, S Ghugal, « Design and Development of a Retrofit Solution for Converting a Conventional LCV into Parallel Hybrid Electric Vehicle », *Symposium on International Automotive Technology 2019*, January. 2019, pp. 2019-26-0117, doi: 10.4271/2019-26-0117.

[4] C. C. Chan, A. Bouscayrol, K. Chen, "Electric, Hybrid and Fuel Cell Vehicles: Architectures and Modeling", IEEE transactions on Vehicular Technology, vol. 59, no. 2, pp. 589-598, February 2010

[5] Englisch, Andreas & Pfund, Thomas & Reitz, Dierk & Simon, Emmanuel & Kolb, Florian. (2017). Synthesis of various hybrid drive systems.

[6] A. Bouscayrol, J. P. Hautier, B. Lemaire-Semail, "Graphic Formalisms for the Control of Multi-Physical Energetic Systems", *Systemic Design Methodologies for Electrical Energy, tome 1, Analysis, Synthesis and Management, Chapter 3*, ISTE Willey editions, October 2012, ISBN: 9781848213883

[7] J.P. Hautier, P.J. Barre, « The causal ordering graph – A tool for modeling and control law synthesis", *Studies in Informatics and Control Journal*, vol. 13, no. 4, pp. 265-283, 2004.

[8] T. Letrouve, A. Bouscayrol, W. Lhomme, N. Dollinger, et F. M. Calvairac, « Different models of a traction drive for an electric vehicle simulation », IEEE-VPPC'10, Lille, France, September 2010, doi: 10.1109/VPPC.2010.5729209.

[9] J. G. Hayes and G. A. Goodarzi, 'Electric Powertrain: Energy Systems, Power Electronics and Drives for Hybrid, Electric and Fuel Cell Vehicles',WILEY,2018

[10] Mehrdad Ehsani, Yimin Gao, Stefano Longo, and Kambiz M. Ebrahimi, Modern Electric, Hybrid Electric, and Fuel Cell Vehicles, Third Edition. CRC Press, 2018

[11] S. G. Wirasingha et A. Emadi, « Classification and Review of Control Strategies for Plug-In Hybrid Electric Vehicles », *IEEE Trans. Veh. Technol*, vol. 60, no.º 1, pp. 111-122, January. 2011, doi: 10.1109/TVT.2010.2090178.

[12] R. Ghorbani, E. Bibeau, et S. Filizadeh, « On Conversion of Hybrid Electric Vehicles to Plug-In », IEEE Trans. Veh. Technol., vol. 59, nº 4, p. 2016-2020, mai 2010, doi: 10.1109/TVT.2010.2041563.

[13] V. Wynen, F.-S. Boureima, J. Matheys, P. Bossche, et J. Van Mierlo, « Developing applicable driving cycle for retrofitted Plug-In Hybrid ElectricVehicles (PHEVs): environmental impact assessment », WEVJ, vol. 3, nº 1, p. 147-159, mars 2009, doi: 10.3390/wevj3010147.

[14] *U.S. Energy Information Administration*. Accessed on: August 19, 2020. [Online]. Available: https://www.eia.gov

Appendix: EMR Pictograms